UCRL-JC-121992
PREPRINT

CONF-9409153--4

Characterization of Vanadium/Silica and Copper/Silica Aerogel Catalysts

L. Owens
T.M. Tillotson
L.M. Hair

This paper was prepared for submittal to the
Fourth International Symposium on Aerogels (ISA-4)
in Berkeley, CA. on Sept. 19-21, 1994
and
Journal of Non-Crystalline Solids

September 1995

Lawrence Livermore National Laboratory

DISCLAIMER

Characterization of Vanadium/Silica and Copper/Silica Aerogel Catalysts

L. Owens, T.M. Tillotson, and L.M. Hair
Chemistry & Materials Science Department
Lawrence Livermore National Laboratory
Livermore, CA 94550

Abstract

Vanadium/silica and copper/silica aerogels have been prepared using the sol-gel method followed by CO_2 exchange and supercritical extraction. Structural properties of samples supercritically dried, oxidized and used in reactions studies conducted with a feed representing the average composition of automobile exhaust from a lean burn engine were investigated using laser Raman spectroscopy and temperature-programmed reduction. No evidence of crystalline V_2O_5 was found for the vanadium/silica aerogel, freshly extracted, oxidized or following exposure to reaction conditions using these techniques. However, results obtained for the copper/silica sample indicate that changes in the structure of the copper species had occurred as the sample was oxidized and exposed to reaction conditions.

1. Introduction

Vanadia supported on metal oxides and copper based zeolites have been shown to be useful for the reduction of NO_x in heterogeneous catalytic processes (1,2). As concerns for the environment increase, the need for stable, high surface area catalysts with these components increases. Dispersing active metal oxide components on metal oxide supports such as SiO_2, Al_2O_3, and TiO_2, or in zeolites increases active surface area of metal oxide components. In many cases, the dispersed metal oxide phases have also been shown to be more selective than bulk oxides (3-5). However, aggregation or sintering of active components may occur as a result of high temperature oxidation and exposure to reaction conditions. Using the aerogel synthesis to prepare metal oxide catalysts offers the advantage of producing high surface area materials with good dispersions and high thermal stability.

In this investigation, we have studied the structural properties of vanadium/silica and copper/silica aerogels as a function of exposure to oxidizing conditions and in reaction studies using laser Raman spectroscopy and temperature-programmed reduction (TPR).

Work performed under the auspices of the U.S. Department of Energy by the Lawrence Livermore National Laboratory under Contract W-7405-Eng-48.

Laser Raman spectroscopy has been shown to be a useful tool in elucidating structural characteristics of dilute supported metal oxide systems (6-8). In particular, dispersed vanadia species have been found to be easily distinguishable from crystalline V_2O_5. More recently, TPR has been found to be useful in studying the dispersion of metal oxides in supported systems when used with a second complementary technique (10).

2. Experimental

2.1 BET Surface Area, Pore Structure Analysis, and Elemental Analysis

Sample preparation is described elsewhere (11). Aerogel samples as prepared from the extraction vessel, and subsequently oxidized at 400°C for 2 hours to remove remaining organic compounds and exposed to the reaction conditions described below were labeled CuSiAP and VSiAP, CuSiOxy and VSiOxy, and CuSiAR and VSiAR, respectively.

Surface area and pore size distribution analyses were conducted on a Micromertics ASAP 2000 gas adsorption analyzer. Prior to the analyses, samples were outgassed under vacuum (10^{-5} torr) and at 50°C (CuSiAP and VSiAP) or 100°C (CuSiOxy, VSiOxy, CuSiAR, and VSiAR) for a minimum of 8 hours. Sample compositions were determined using inductively-coupled plasma atomic emission spectroscopy.

2.2 Temperature-programmed reduction (TPR)

TPR experiments were carried out in a quartz microreactor in a continuous flow system with a feed stream of 5 % H_2 in argon at a flow rate of 60 ml/min using a heating rate of 5°C/min to 800°C. The samples were pretreated at 400°C in a flow of pure O_2 at 80-90 ml/min for 45 minutes. The consumption of hydrogen from the feed stream was detected using a Gowmac thermal conductivity detector (WX) at 100°C. The water produced by reduction was removed by a molecular sieve trap after the reactor and upstream of the TCD. Peak maxima were recorded within ±5°C. Peak areas were determined using the software application KaleidaGraph.

2.3 Laser Raman Spectroscopy

Laser Raman Spectra were collected using the 488 nm line of a Spectra-Physics Ar ion laser (Model 165). A Spex 0.75 meter double spectrograph (Model 1400) with a 300 g/mm grating was used with a Princeton Instruments liquid nitrogen cooled, front illuminated CCD detector. The Raman spectrum collected from approximately 2200 to 200 cm^{-1} was calibrated with a toluene or bulk V_2O_5 spectrum. Laser Powers of 50 and 150 mW were used for the aerogel and bulk oxide samples, respectively. Spectra were collected in air for 20 to 300 seconds on pellets pressed from approximately 0.01 g of sample.

2.4 Reaction Studies

Reactions were carried out in a quartz microreactor. The total flow rate was 200 ml/min with a feed composition of propane (175 ppm), hydrogen (130 ppm), carbon monoxide (400 ppm), propylene (525 ppm), carbon dioxide (7.0 volume %), nitric oxide (230 ppm), and oxygen (8.00 volume %) in a balance of helium. Samples were oxidized in pure oxygen at 400°C for 30 minutes prior to reaction. Approximately 0.2 g of sample was used in each experiment. A thermocouple inside the catalyst bed was used to record the reaction temperature. Product gases were analyzed with an on-line mass spectrometer (Questor) and a NO/NO_x analyzer (Teledyne, Model 912). The products detected were methane, water, carbon monoxide, oxygen, propane, propylene, carbon monoxide, and a combination of nitric oxide and nitrogen dioxide. Conversions were defined as the percentage of the component in the feed which had reacted and were recorded within ±3% conversion.

3. Results

Table 1 lists the composition, BET surface area, and pore volume and diameter, and Figure 1 shows the pore size distribution of the samples studied. The copper loading in the aerogel samples corresponded to the amount of copper acetate added during preparation. However, the vanadium in the aerogel samples was one-third of the value expected based on the amount of vanadium tri-isopropoxide added indicating that some of the precursor had been lost most likely during the CO_2 exchange process. The surface area, total pore volume, and average pore size decreased as the extracted sample was oxidized and then exposed to reaction conditions. Figure 2 shows results of the reaction studies. Over the temperature range studied, maximum NO conversions for VSiOxy and CuSiOxy were approximately 10 and 20 %, respectively.

CuSiAP and CuSiOxy were light blue. CuSiAR was non homogeneous having a base color of green with dark brown specks. VSiAP was red-orange after extraction and turned dark green over time when exposed to air. VSiOxy was dark orange while VSiAR was white immediately after reaction in the reactor before exposure to the atmosphere and turned dark orange upon exposure to air.

3.1 *Vanadium/silica*

Figure 3 shows the TPR profiles of the VSiOxy, VSiAR, and bulk V_2O_5. The profiles of VSiOxy and VSiAR exhibit one peak at T = 530°C (Figure 3B, D) while the profile of bulk V_2O_5 exhibits three distinct peaks at T = 675, 705, and 845°C (Figure 3A). The profile of the second TPR experiments of VSiOxy also shows one peak (Figure 3C). However, the peak maximum has shifted to T = 545°C.

Analysis of the peak areas was conducted to determine the amount of vanadium reduced during the TPR experiment. The consumption of hydrogen was determined using the peak area obtained from the reduction of CuO for reference. The results obtained show that 95-100% of the vanadium in the bulk V_2O_5 was reduced from V^{5+} to V^{3+} while approximately 80% of the vanadium in VSiOxy and VSiAR was reduced from V^{5+} to V^{3+} in each TPR experiment.

The laser Raman spectra of bulk V_2O_5, VSiAP, VSiOxy, and VSiAR is shown in Figure 4. Features at approximately 998, 704, 526, 484, 404, 304, and 284 cm^{-1} were present in the spectrum of bulk V_2O_5. No peaks indicating the presence of crystalline V_2O_5 were observed in the spectra of VSiAP, VSiOxy, or VSiAR (Figure 4B-D). However, a feature at approximately 1040 cm^{-1} and a broad peak at 490 cm^{-1} were observed.

3.2 *Copper/silica*

Figure 5 shows the TPR profiles of CuSiOxy, bulk CuO, and CuSiAR. The profile of CuSiOxy exhibits two peaks at T = 210 and 440°C (Figure 5B). The profile of bulk CuO exhibits one peak at T = 288°C (Figure 5A). One peak at T = 210°C was observed in the profile of the second TPR experiment of CuSiOxy (Figure 5C) and in the profile of CuSiAR (Figure 5D).

Unfortunately, analysis of the peak areas for CuSiOxy and CuSiAR yielded high uncertainty in determination of peak areas. However, comparison of the ratios of the peak areas of the first and second peak in the profile of CuSiOxy indicate that 60-65% of the total peak area was under the first peak while the remaining 35-40 % was under the second.

The laser Raman spectra of the bulk copper oxides, CuO and Cu_2O, and CuSiAP, CuSiOxy and CuSiAR are shown in Figure 6. A feature at 660 cm^{-1} was observed in the spectrum of the CuO (Figure 6A). Strong features at approximately 640 and 215 cm^{-1} and weak broad features at approximately 410 and 500 cm^{-1} were observed in the spectrum of Cu_2O (Figure 6B). No peaks were observed in the spectrum of CuSiAP (Figure 6C). The spectrum of CuSiOxy exhibits features at 970, 810, and 490 cm^{-1}. Figure 6E shows the spectrum of CuSiAR. Similar to the spectrum of CuSiOxy, features were observed at 970, 810, 490 cm^{-1}. However, additions features at 660 and 600 cm^{-1} were also observed.

4. Discussion

4.1 Vanadium/silica

Raman spectra of VSiAP, VSiOxy and VSiAR exhibited no peaks corresponding to crystalline V_2O_5. However, a feature which has been previously attributed to an isolated monomeric surface vanadyl species, $(Si\text{-}O\text{-})_3 \int V = O$ was observed (6-8). In this species, the V ion is in the tetrahedral coordination, and the frequency of the stretching vibration of the V=O is approximately 1040 cm^{-1}. This peak has been shown to be affected reversibly by the hydration-dehydration process which supports its assignment as a surface species (6,7). The assignment of this monomeric surface species to 1040 cm^{-1} has been consistent in the laser Raman spectra of silica-supported vanadia samples collected under controlled atmospheres in the absence of water vapor (9). The observation of this feature in this investigation could be a result of water desorption due to heat generated by the laser during the experiment.

Temperature programmed reduction profiles of VSiOxy and VSiAR exhibit one reduction peak more than 100°C lower than the first of three reduction peaks for V_2O_5. Similar results have been reported for silica-supported vanadia samples where the vanadia species present as two dimensional surface species were found to reduce at lower temperatures than bulk oxides as a result of their orientation and high accessibility for reduction (10,12). Koranne et al.(10) and Roozeboom et al.(12) observed multiple reduction peaks for samples which contained vanadia with more than one coordination. Thus, a change in structure would yield a shift in the reduction peak in the TPR profile as was observed in the profile of VSiOxy in the second TPR experiment (Figure 5C). Similarities in the TPR profiles of VSiOxy and VSiAR indicate that the structural properties of VSiOxy were maintained after oxidation and exposure to reaction conditions.

4.2 Copper/silica

The laser Raman spectra of the copper samples is shown in Figure 6. In addition to the feature at 660 cm^{-1} observed in Figure 6A, features at 296 and 345 cm^{-1} have been previously reported for bulk CuO (13), but were masked under a steep, broad feature of our spectrum (Figure 6A). Features at 640, 500, 410, and 215 cm^{-1} observed in the spectrum of Cu_2O (Figure 6B) has also been previously reported (13). Features at 970, 810, and 490 cm^{-1} were observed in the spectrum of CuSiOxy (Figure 6C). However, no peaks corresponding to crystalline CuO were observed. Igarashi et al.(14) studied silica aerogels with laser Raman spectroscopy and observed features at 440, 490, 810 and 970 cm^{-1} as well as a peak observed at 600 cm^{-1} with increasing calcination temperatures. Thus, these features in the spectrum of CuSiOxy (Figure 6C) were attributed to the silica aerogel. In addition to features at 490, 810, and 970 cm^{-1} attributed to the silica aerogel in the spectrum of CuSiAR (Figure 6E), the feature at 660 cm^{-1} indicated the formation of crystalline CuO with exposure to reaction conditions. The appearance of the feature at 600 cm^{-1} attributed to the silica aerogel also indicated a change in the silica structure as well.

TPR profiles for CuSiOxy contain two reduction peaks. The first occurred at a temperature 80°C lower than the single reduction peak of CuO representing a highly dispersed copper oxide species. Similarly, van der Grift et al.(15) have studied silica-supported copper samples and found that well-dispersed copper oxide reduced more easily than bulk CuO. They studied three copper silicate compounds using TPR and observed multiple reduction peaks, and reduction peaks at higher temperatures than those observed in the TPR profiles of CuO and silica-supported copper samples indicating that the copper silicate compounds were harder to reduce than dispersed and bulk CuO. In this investigation, the second high temperature reduction peak observed in the TPR profile of CuSiOxy (Figure 5C) represents a copper species which is harder to reduce than dispersed copper oxide. During of the aerogel synthesis, it is possible that a copper species with bonds to silica (- Cu - O - Si -) or a copper silicate compound may be formed during the gellation or oxidation process. However, comparison of the TPR profiles of the copper silicates (15) to those in this study is difficult due to the difference in experimental conditions which greatly affect the location and shape of peak maxima (16). Thus, further experiments are needed to confirm the presence of copper silicate compounds in these samples. When a second TPR experiment was conducted on CuSiOxy (Figure 5D), the second reduction peak disappeared and the area under the first peak increased indicating that the structure of the copper species represented by the high temperature was not reformed during the oxidation step before the second TPR. Similarly, after exposure to reaction conditions the second high temperature reduction peak had disappeared from the TPR profile of CuSiAR. The results of the TPR and laser Raman experiments, and the change in physical appearance of the sample indicate that the structure of the copper species in the copper/silica aerogel had changed under reaction conditions such that highly dispersed crystalline CuO was formed at the expense of an unknown copper species represented by the high temperature reduction peak in the TPR profile of CuSiOxy.

5. Conclusions

Vanadium/silica and copper silica aerogels were studied with laser Raman spectroscopy and temperature-programmed reduction. Changes in the structural properties of the vanadium/silica aerogels after oxidation or upon exposure to reaction conditions were not distinguishable using temperature-programmed reduction and laser Raman spectroscopy.

Highly dispersed vanadia surface species were present in these samples. Results obtained from both Raman spectra and TPR profiles indicate that structural changes occurred in the copper/silica aerogels when oxidized and exposed to reaction conditions. Highly dispersed copper oxide species were present in the extracted and oxidized sampled while the formation of well-dispersed crystalline CuO was detected in the copper/silica aerogel after reaction.

Acknowledgments

The authors would like to thank Kevin Kyle and Eric Mayes for assistance with the laser Raman experiments, and Suzanne Hulsey and Cindy Alviso for conducting the N_2 adsorption and desorption experiments.

References

1. Baiker, A., Dollenmeier, P., Glinski, M., and Reller, A., Appl. Catal., 35 (1987) 351.

2. Iwamoto, M., Yokoo, S., Sakai, K., and Kagwa, J. Chem. Soc., Faraday Trans. 1, 77 (1981) 1629.

3. Oyama, S.T., and Somorjai, G.A., J. Phys. Chem., 94 (1990) 5022.

4. Le Bar, J., Auroux, A., and Vedrine, J.C., Stud. Surf. Sci. Catal., 72 (1992) 181.

5. Owens, L., and Kung, H.H., J. Catal., 144 (1993) 202.

6. Miyata, H., Tokunda, S., and Yoshida, T., Appl. Spectrosc., 43 (1989) 522.

7. Oyama, S.T., Went, G.T., Lewis, K.B., Bell, A.T., and Somorjai, G.A., J. Phys. Chem., 93 (1989) 6786.

8. Went, G.T., Oyama, S.T. and Bell, A.T., J. Phys. Chem., 94 (1990) 4240.

9. Oyama, S.T., Res. Chem. Intermed., 15 (1991) 165.
10. Koranne, M.M., Goodwin, J.G., and Marcelin, G., J. Catal., 148 (1994) 369.

11. Hair, L.M., Owens, L., Tillotson, T., Froeba, M., Wong, J., Thomas, G.J., and Medlin, D.L., in this proceedings.

12. Roozeboom, F., Mittelmeijer-Hazeleger, M.C., Moulijn, J.A., Medema, J., de Beer, V.H.J., and Gellings, P.J., J. Phys. Chem., 84 (1980) 2783.

13. Kilo, M., Schild, C., Wokaun, A., and Baiker, A., J. Chem. Soc. Faraday Trans. 1, 88 (1992) 1453.

14. Igarashi, K., Tajiri, K., Tai, Y., and Tanemura, S., Supplement to Z. Phys. D, 26 (1993) S207.

15. van der Grift, C.J.G., Mulder, A., and Geus, J.W., Appl. Catal., 60 (1990) 181.

16. Fierro, G., Lo Jacono, M., Inversi, M., Porta, P., Lavecchia, R., and Cioci, F., J. Catal., 148 (1994) 709.

Table 1: Summary of Physical Characteristics

Sample	Description	Cu wt.%	V wt.%	BET Surface Area m^2/g	Total Pore Volume (cc/g)	Average Pore Diameter (Å)
CuSiAP	As prepared[a]	3.1	-	591	1.06	61.5
CuSiOxy	Oxidized at 400°C	2.8	-	583	1.03	59.9
CuSiAR	After Reaction[b]	3.2	-	565	0.97	57.8
VSiAP	As prepared[a]	-	3.8	530	1.18	78.7
VSiOxy	Oxidized at 400°C	-	3.9	501	1.12	76.7
VSiAR	After Reaction[b]	-	4.3	462	1.09	73.8

a) After CO_2 extraction
b) See reaction studies for conditions

Figure 1: Pore volume (cc/g) versus pore diameter (Å) for A) Vanadium/silica aerogels and B) Copper/silica aerogels.

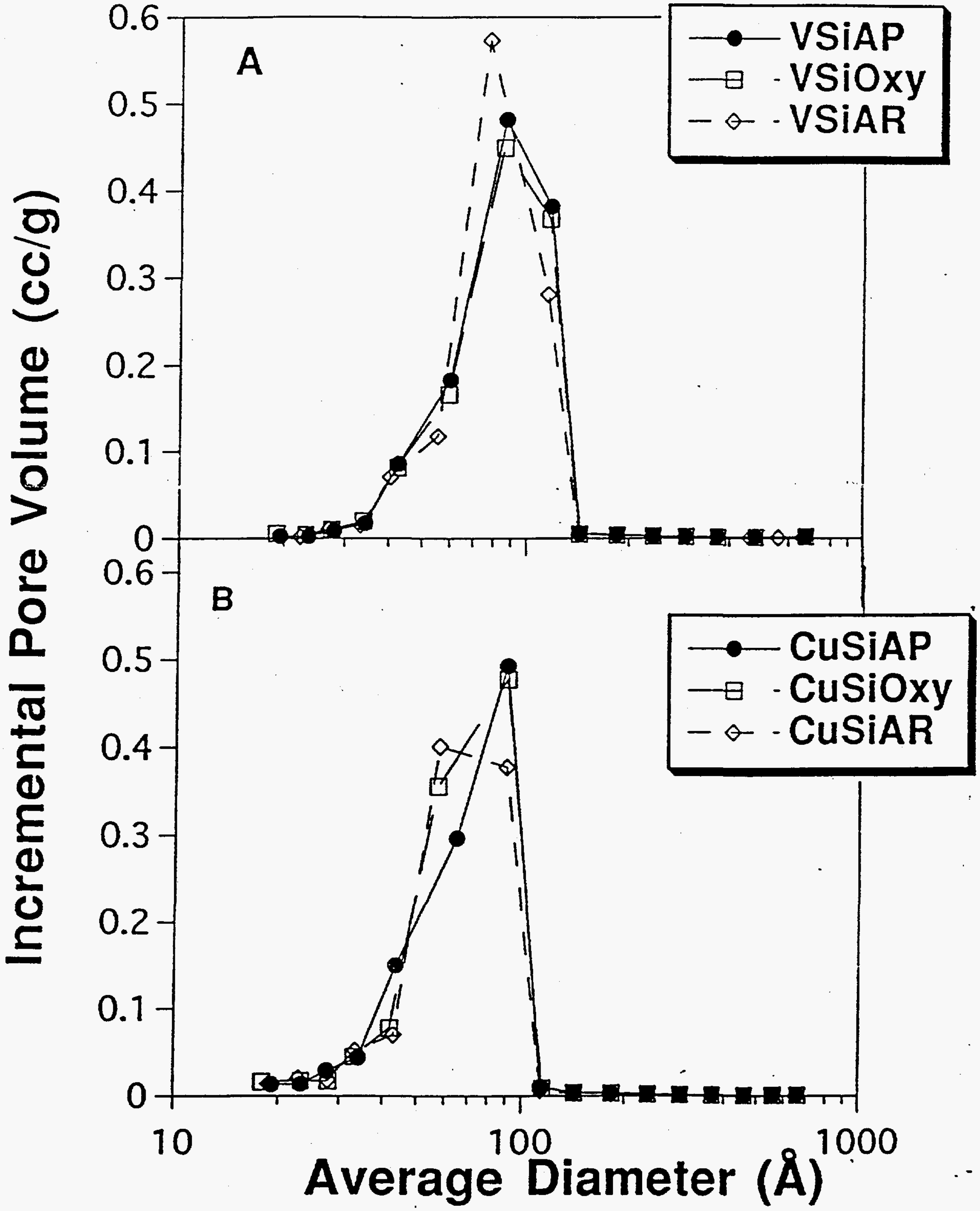

Figure 2: NO, C_3H_6, and C_3H_8 conversion for A) VSiOxy and B) CuSiOxy.

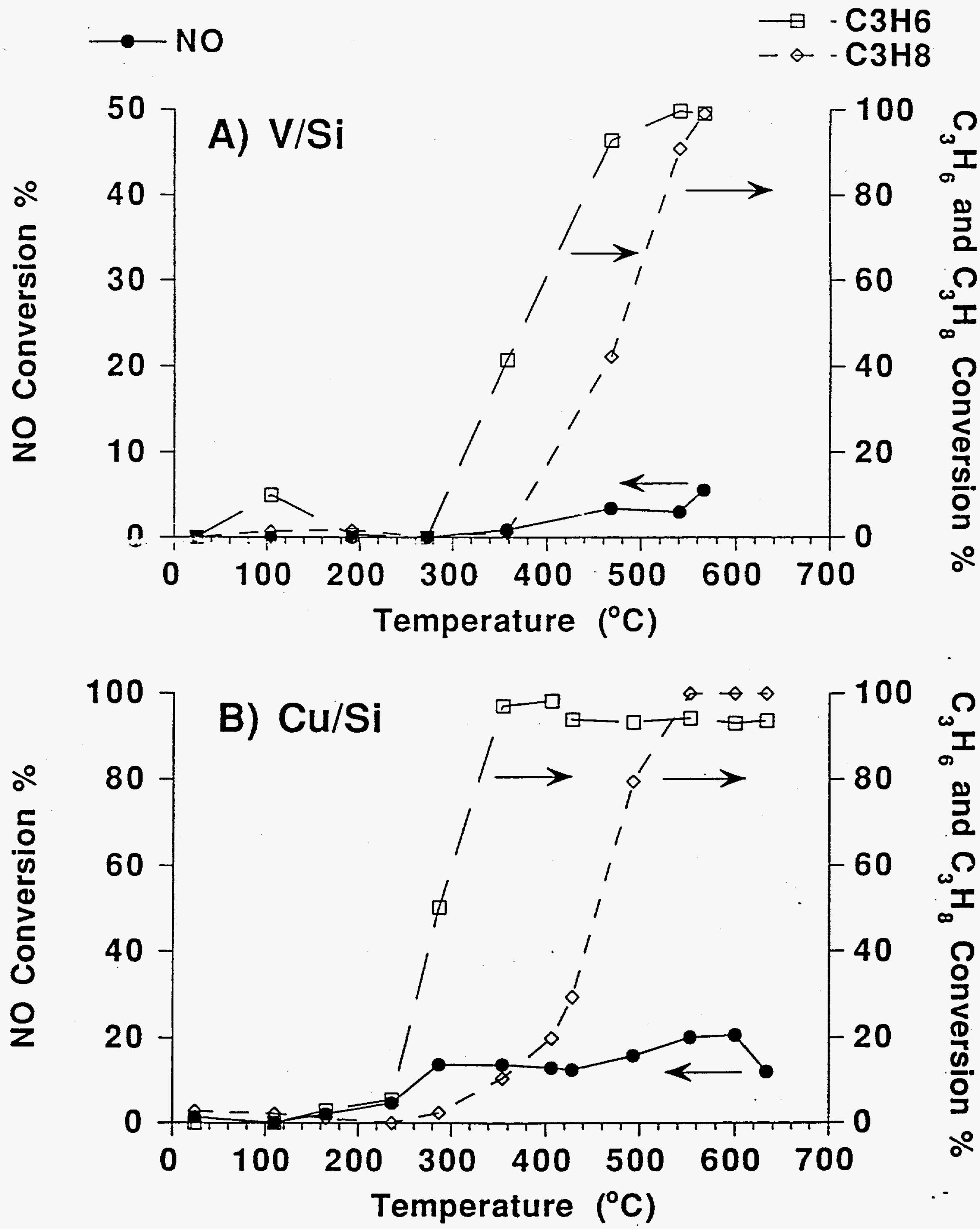

Figure 3: Temperature-programmed reduction profiles of A) Bulk V_2O_5, B) VSiOxy, C) VSiOxy 2nd TPR, and D) VSiAR. A feed of 5% H_2 in argon with a flow rate of 60 ml/min, and a heating rate of 5°C/min was used. Samples were pretreated in a flow of pure O_2 at 80-90 ml/min for 30-45 minutes at 400°C.

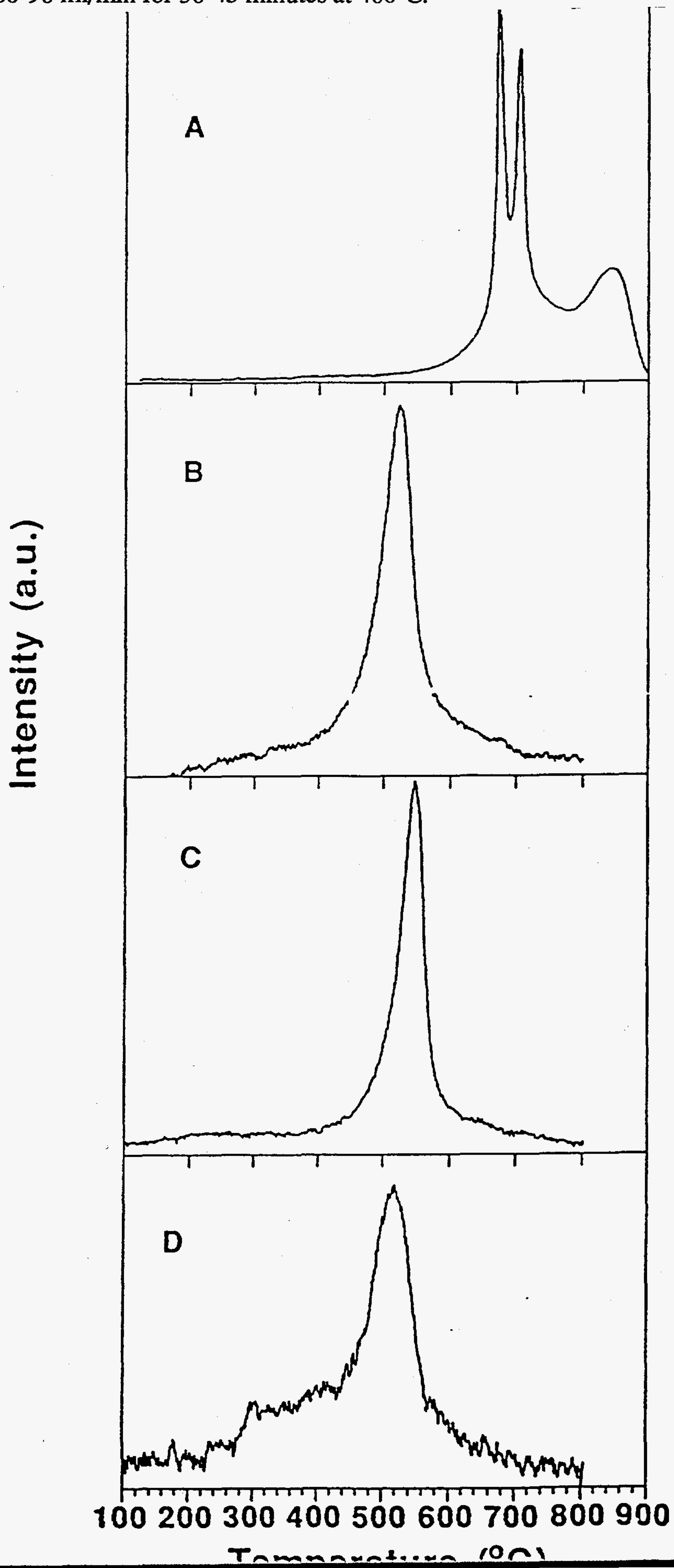

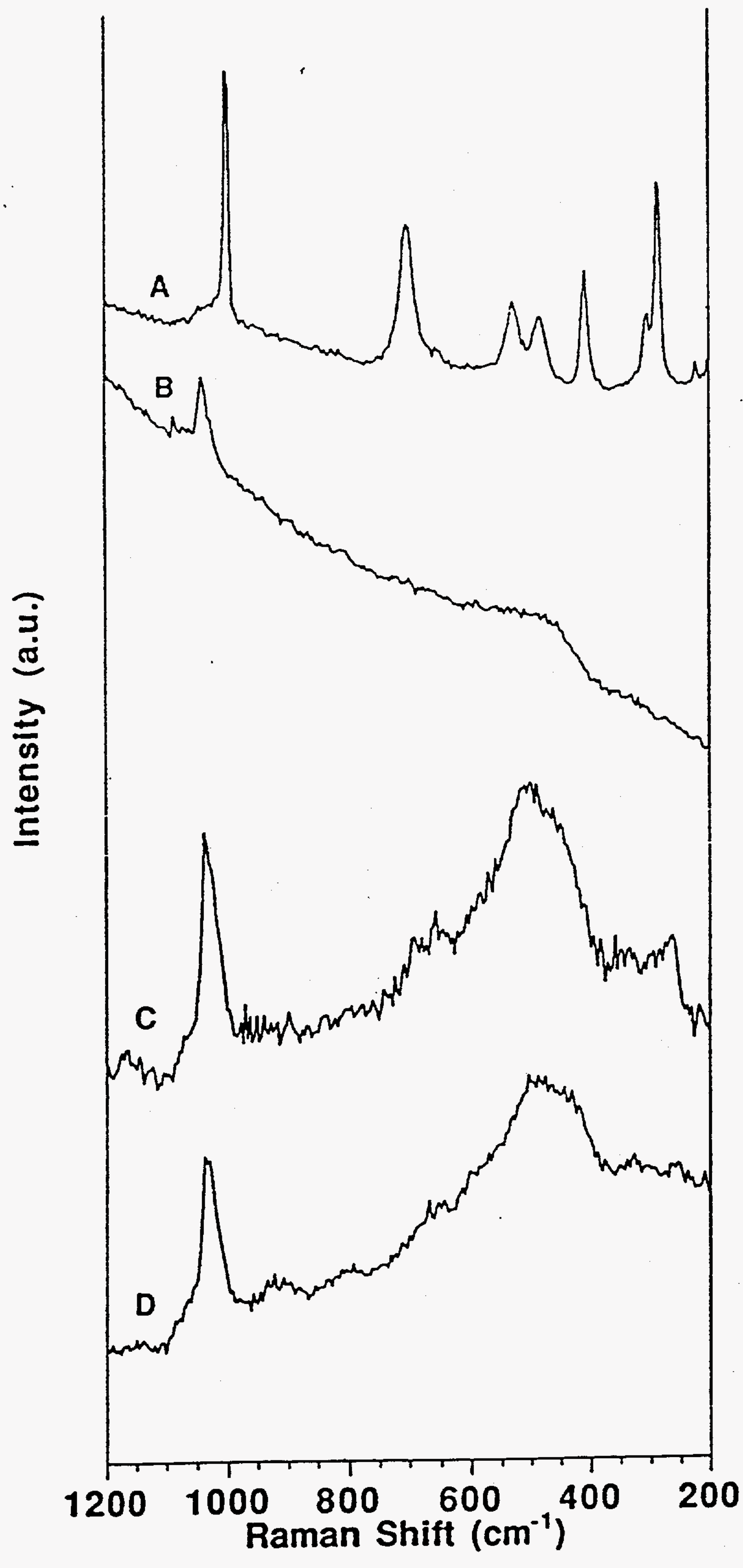

Figure 4: Laser Raman spectra of A) Bulk V_2O_5, B) VSiAP, C) VSiOxy, and D) VSiAR. A laser power of 50 mW and collection times from 30-60 seconds were used.

Figure 5: Temperature-programmed reduction profiles of A) Bulk CuO, B) CuSiOxy, C) CuSiOxy 2nd TPR, and D) CuSiAR. A feed of 5% H_2 in argon with a flow rate of 60 ml/min, and a heating rate of 5°C/min was used. Samples were pretreated in a flow of pure O_2 at 80-90 ml/min for 30-45 minutes at 400°C.

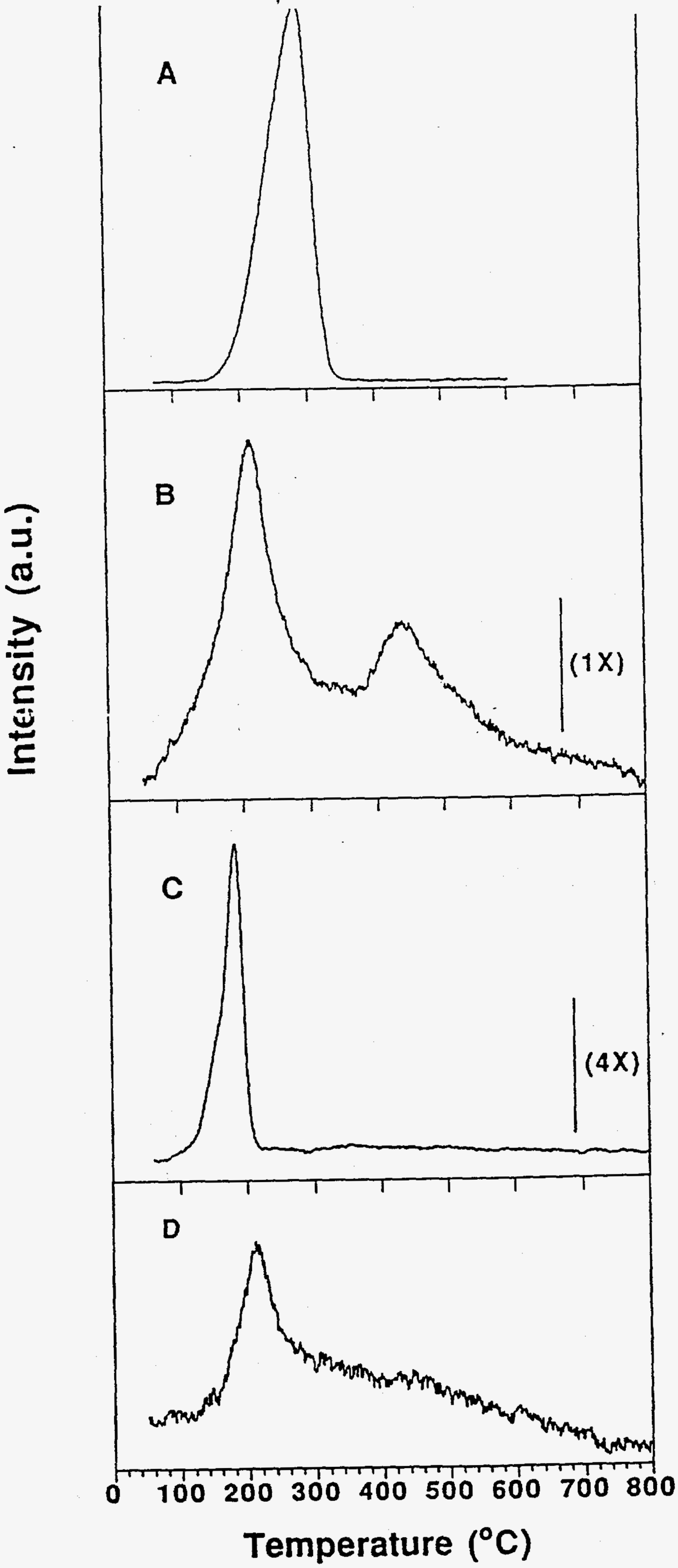

Figure 6: Laser Raman spectra of A) Bulk CuO, B) Bulk Cu_2O, C) CuSiAP, D) CuSiOxy, and E) CuSiAR. A laser power of 150 mW and collection times from 120-300 seconds were used for the CuO and Cu_2O, and 50 mW and 30-60 seconds were used for CuSiAP, CuSiOxy, and CuSiAR.